

Electronic Supplementary Information (ESI)

Highly Efficient Uptake into Cisplatin-Resistant Cells and the Isomerization upon Coordinative DNA binding of Anticancer Tetrazolato-Bridged Dinuclear Platinum(II) Complexes

Masako Uemura, Miyuu Hoshiyama, Ayako Furukawa, Takaji Sato, Yoshihiro Higuchi, and Seiji Komeda

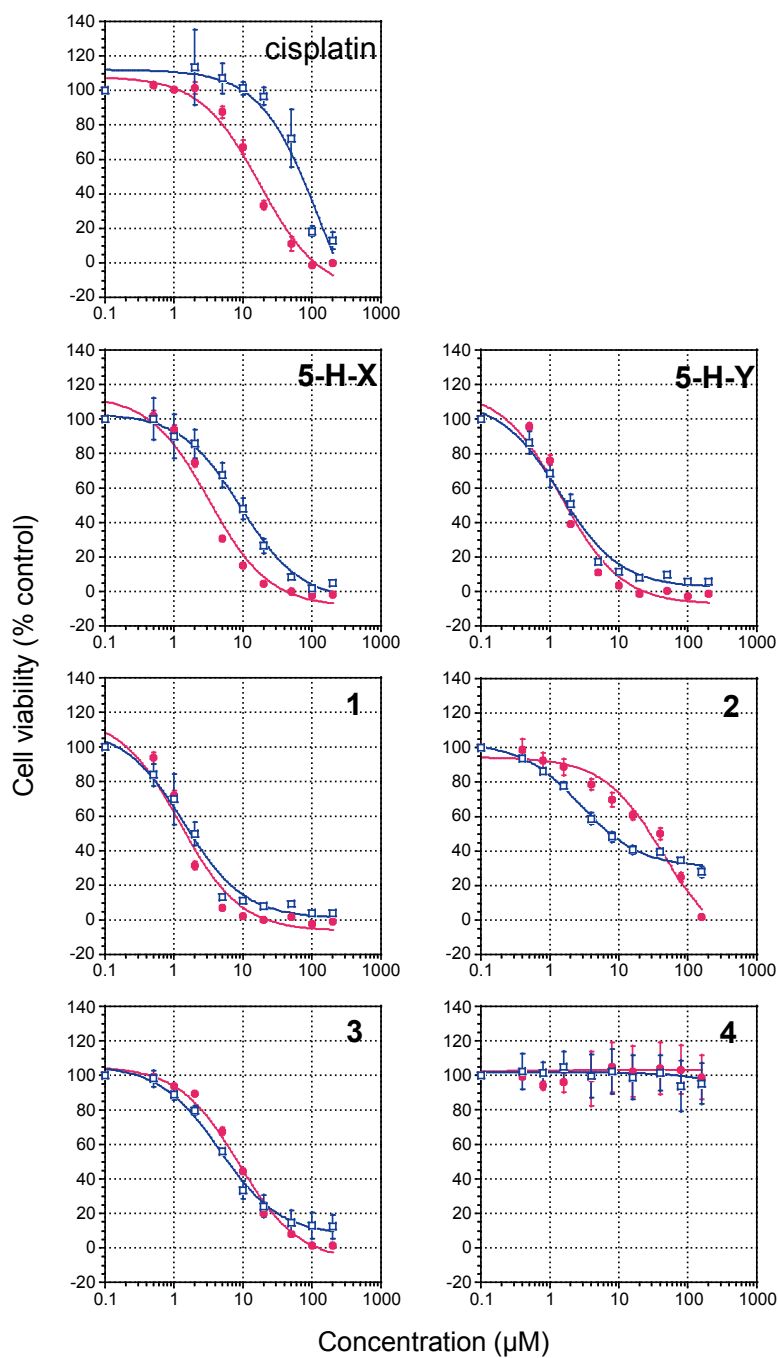


Fig. S1 Dose–response curves for cell viability obtained by means of an MTT assay. L1210 cells (●) and L1210R cells (□). Curve fittings were conducted with the KaleidaGraph graphing and data analysis software. Results are presented as the mean ± standard deviation from four experiments. On the x-axis, 0.1 µM is equal to 0 µM. Tetrazolato-bridged dinuclear platinum(II) complexes: [*cis*-Pt(NH₃)₂}(μ-OH)(μ-tetrazolato-*N1,N2*)]²⁺ (**5-H-X**) and [*cis*-Pt(NH₃)₂]₂(μ-OH)(μ-5-R-tetrazolato-*N2,N3*)]ⁿ⁺, where R = H (**5-H-Y**), CH₃ (**1**), C₆H₅ (**2**), CH₂COOCH₂CH₃ (**3**), or CH₂COO⁻ (**4**), and n = 2 (**5-H-Y**, **1–3**) or 1 (**4**).

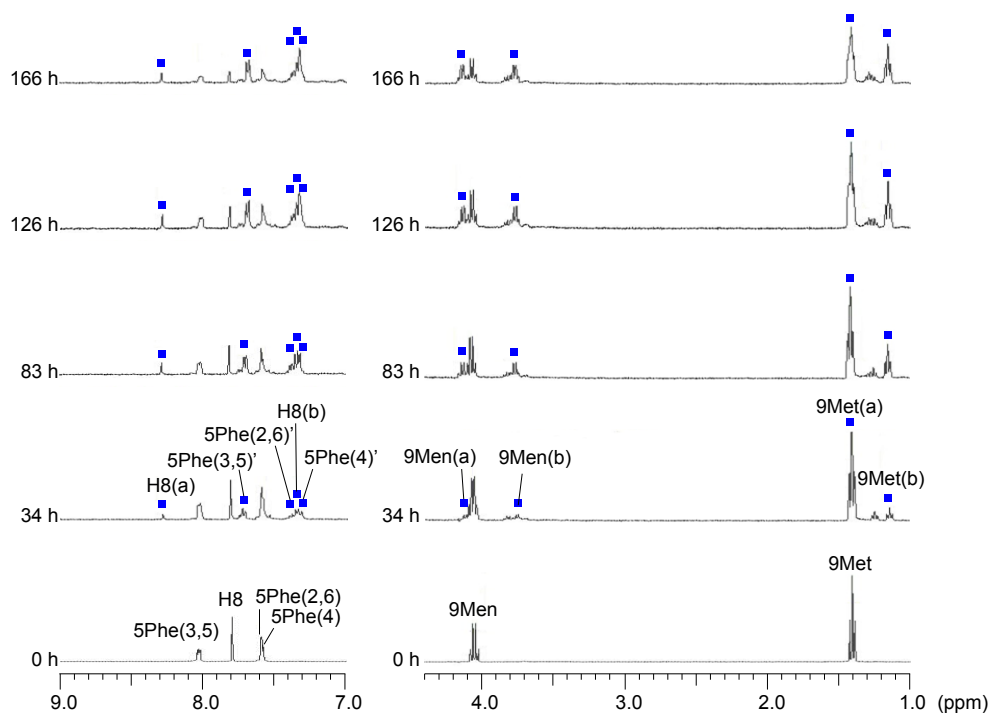
A

Fig. S2 $^1\text{H-NMR}$ spectra of the aromatic and aliphatic regions in the reactions of **2–4** (A–C) with two molar equivalents of 9EtG at 37 °C. Each symbol shows the signals of the 9EtG ligands (H8(a) or H8(b)) and the substituent signals at the tetrazolate C5 in the corresponding 1 : 2 complexes; **II–IV** (■). The open blue square (□) in **B** shows the signals of **IV**, which is a hydrolysis product of **III**. Some of the signals of **III** in the aliphatic regions were difficult to assign because they overlapped.

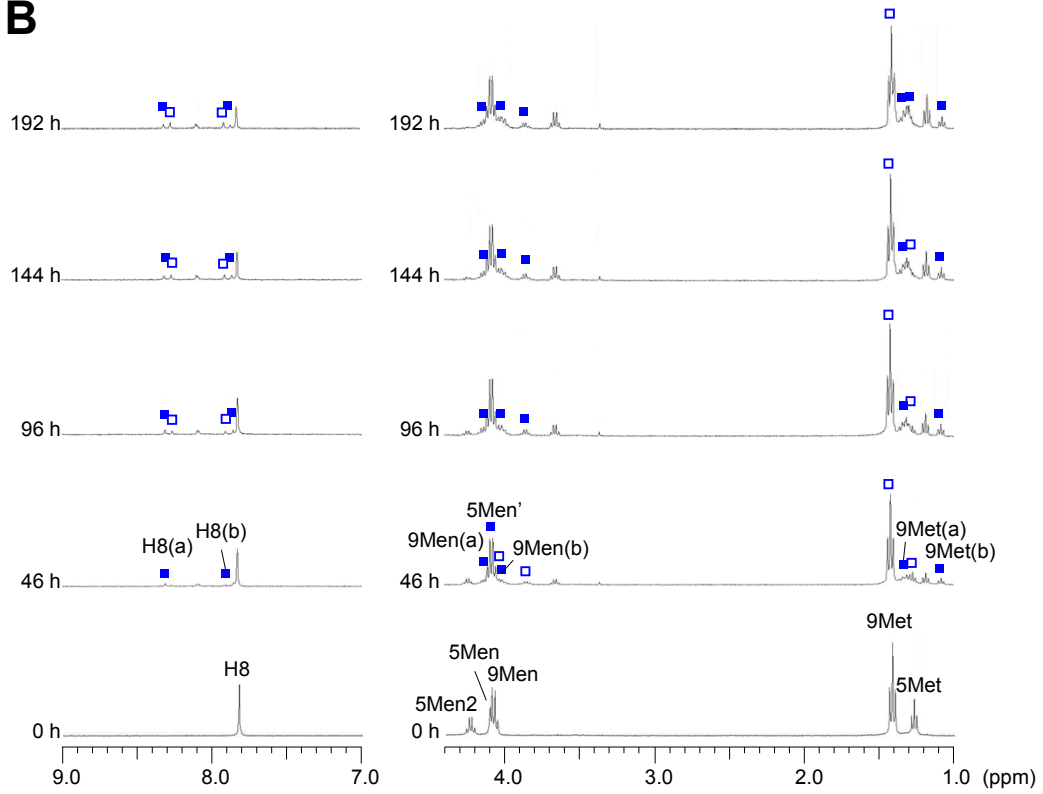
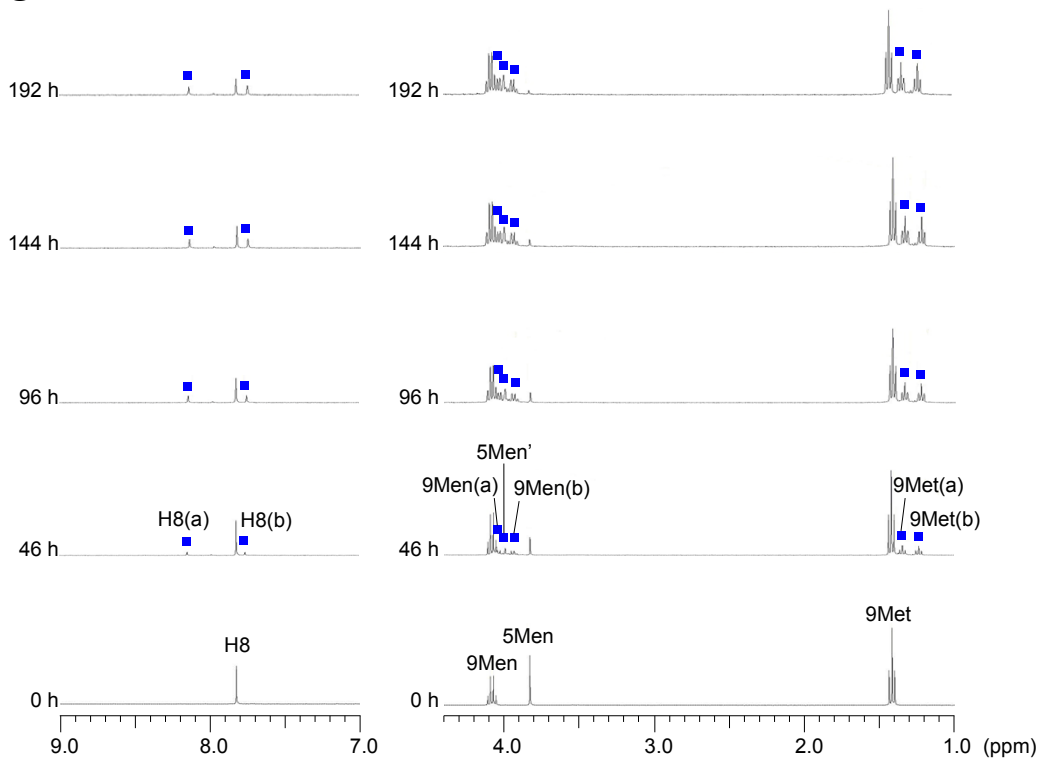
B**C**

Table S1 Results of electron spray ionization mass spectrometry measurements of products obtained from the reactions of **2–4** with two molar equivalents of 9EtG and the exact mass calculated from the predicted empiric formula.

Complex	Molecular formula	Measured accurate mass	Calculated exact mass
1	$[\{cis\text{-Pt}(\text{NH}_3)_2(9\text{EtG-}N7)\}_2(\mu\text{-5-CH}_3\text{-tetrazolato})\text{-NH}_3\text{-2H}]^+$	880.2	880.1907
2	$[\{cis\text{-Pt}(\text{NH}_3)_2(9\text{EtG-}N7)\}_2(\mu\text{-5-C}_6\text{H}_5\text{-tetrazolato})\text{-NH}_3\text{-H}]^{2+}$	471.6	471.6071
3	$[\{cis\text{-Pt}(\text{NH}_3)_2(9\text{EtG-}N7)\}_2(\mu\text{-5-CH}_2\text{COOCH}_2\text{CH}_3\text{-tetrazolato})\text{-NH}_3\text{-H}]^{2+}$	476.6	476.6098
4	$[\{cis\text{-Pt}(\text{NH}_3)_2(9\text{EtG-}N7)\}_2(\mu\text{-5-CH}_2\text{COO}^-\text{-tetrazolato})\text{-NH}_3]^{2+}$	462.6	462.5942

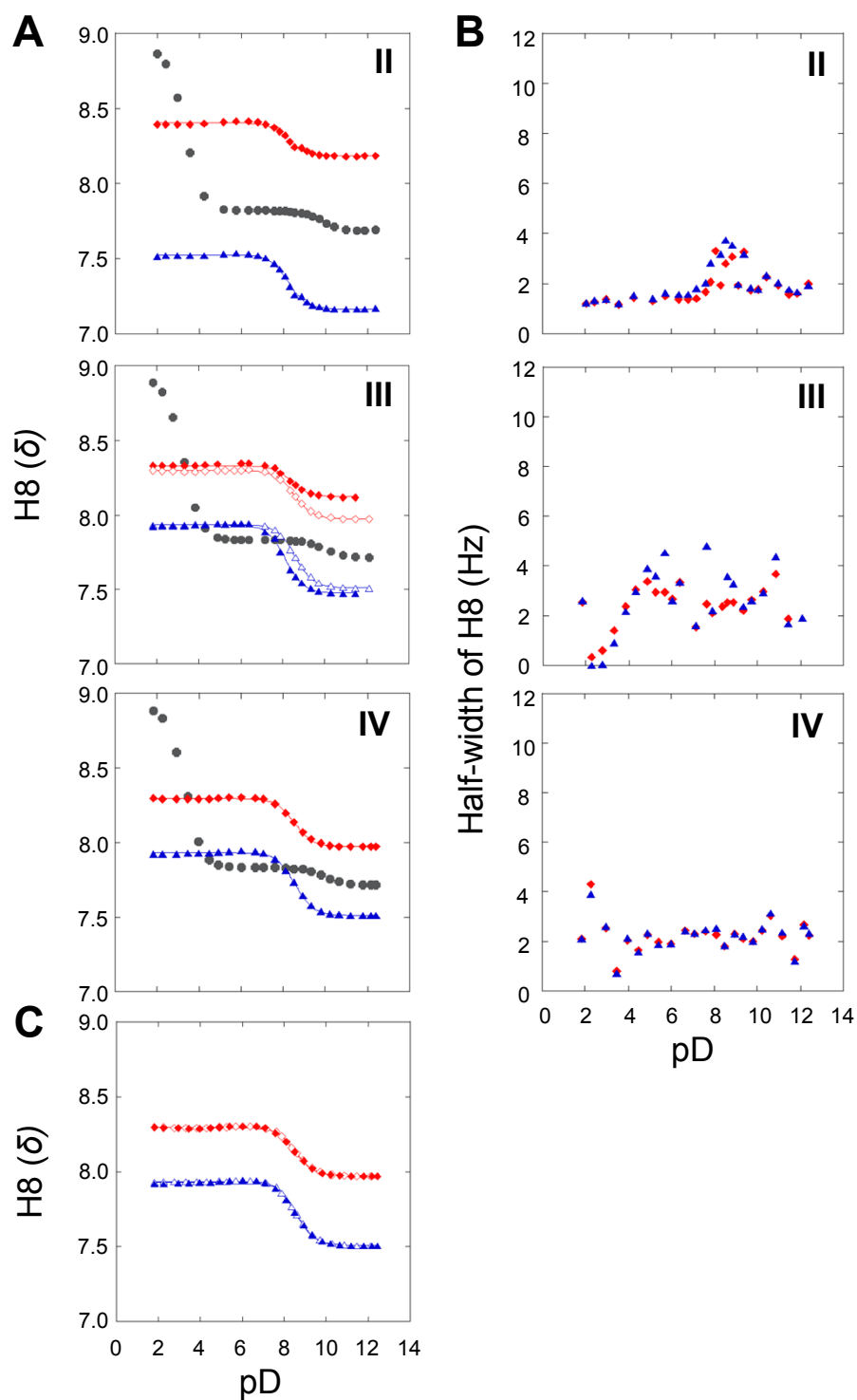


Fig. S3 Plots of pD vs. the chemical shift (A) and half-width (B) of H8 for free 9EtG (●) and H8(a) (◆) and H8(b) (▲) for II–IV. Superimposed plots (C) of III (open red diamonds (◇) and open blue triangles (△)) and IV (◆ and ▲), in which two sets of titration curves were found to be identical, indicating that III is hydrolysed to yield IV.

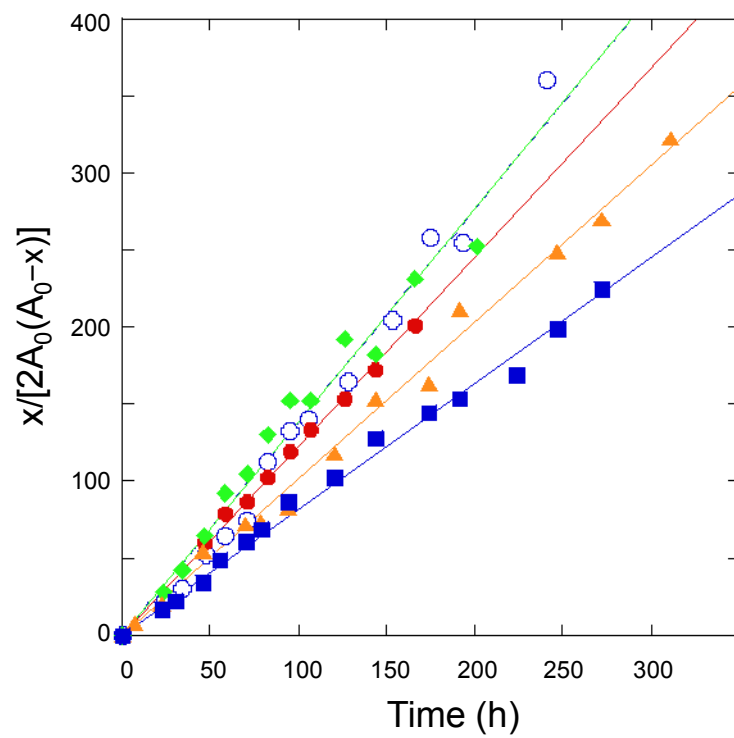


Fig. S4 Second-order Guggenheim plots of the reactions of 5-H-Y (○), 1 (●), 2 (◆), 3 (▲), and 4 (■) with two molar equivalents of 9EtG in D₂O at 37 °C.